Zhou et al. *Zool. Res.* 2023, 44(1): 142−152
https://doi.org/10.24272/j.issn.2095-8137.2022.423

ZR | Zoological Research

Article Open Access

Towards magnetism in pigeon MagR: Iron- and iron-sulfur binding work indispensably and synergistically

Yajie Zhou[1,2], Tianyang Tong[3,2], Mengke Wei[1,2], Peng Zhang[2,4], Fan Fei[2,4], Xiujuan Zhou[2,4], Zhen Guo[5], Jing Zhang[2,4], Huangtao Xu[2], Lei Zhang[2,4], Shun Wang[1,2,4], Junfeng Wang[1,2,4,6], Tiantian Cai[7], Xin Zhang[1,2,4,6], Can Xie[2,4,6,*]

[1] *Institutes of Physical Science and Information Technology*, *Anhui University*, *Hefei*, *Anhui* 230039, *China*

[2] *High Magnetic Field Laboratory*, *Hefei Institutes of Physical Science*, *Chinese Academy of Sciences*, *Science Island*, *Hefei*, *Anhui* 230031, *China*

[3] *Department of Anatomy*, *Anhui Medical University*, *Hefei*, *Anhui* 230032, *China*

[4] *Science Island Branch of Graduate School*, *University of Science and Technology of China*, *Hefei*, *Anhui* 230036, *China*

[5] *School of Life Sciences*, *Peking University*, *Beijing* 100871, *China*

[6] *International Magnetobiology Frontier Research Center*, *Science Island*, *Hefei*, *Anhui* 230031, *China*

[7] *Department of Biological Chemistry and Molecular Pharmacology*, *Harvard Medical School*, 250 *Longwood Avenue*, *Boston*, *MA* 02115, *USA*

ABSTRACT

The ability to navigate long distances is essential for many animals to locate shelter, food, and breeding grounds. Magnetic sense has evolved in various migratory and homing species to orient them based on the geomagnetic field. A highly conserved iron-sulfur cluster assembly protein IscA is proposed as an animal magnetoreceptor (MagR). Iron-sulfur cluster binding is also suggested to play an essential role in MagR magnetism and is thus critical in animal magnetoreception. In the current study, we provide evidence for distinct iron binding and iron-sulfur cluster binding in MagR in pigeons, an avian species that relies on the geomagnetic field for navigation and homing. Pigeon MagR showed significantly higher total iron content from both iron- and iron-sulfur binding. Y65 in pigeon MagR was shown to directly mediate mononuclear iron binding, and its mutation abolished iron-binding capacity of the protein. Surprisingly, both iron binding and iron-sulfur binding demonstrated synergistic effects, and thus appear to be integral and indispensable to pigeon MagR magnetism. These results not only extend our current understanding of the origin and complexity of MagR magnetism, but also imply a possible molecular explanation for the huge diversity in animal magnetoreception.

Keywords: Animal magnetoreception; Iron-sulfur cluster binding; Iron binding; Magnetism; Magnetoreceptor (MagR)

INTRODUCTION

Homing and migration are natural phenomena observed in species across all major phyla in the animal kingdom and display remarkable diversity (Johnsen & Lohmann, 2008; Wiltschko & Wiltschko, 1995; Wiltschko & Wiltschko, 2005).

Received: 18 November 2022; Accepted: 07 December 2022; Online: 08 December 2022

Foundation items: This study was supported by the National Natural Science Foundation of China (31640001 to C.X., U21A20148 to X.Z. and C.X.), and the Presidential Foundation of Hefei Institutes of Physical Science, Chinese Academy of Sciences (Y96XC11131, E26CCG27, and E26CCD15 to C.X.)

*Corresponding author, E-mail: canxie@hmfl.ac.cn

Two fundamentally different forms of information, e.g., direction from polarity and magnetic maps based on intensity and/or inclination, can be derived from the geomagnetic field and play an important role in navigation (Dennis et al., 2007; Heyers et al., 2007; Heyers et al., 2010; Wiltschko & Wiltschko, 1995; Zapka et al., 2009). Several sophisticated theoretical models, including the magnetite-based model (Cadiou & McNaughton, 2010; Kirschvink et al., 2001; Walcott et al., 1979), cryptochrome (Cry)-based radical-pair model (Hore & Mouritsen, 2016; Maeda et al., 2008; Ritz et al., 2000; Rodgers & Hore, 2009), and MagR/Cry-based biocompass model (Lohmann, 2016; Qin et al., 2016; Xie, 2022), have been proposed to explain how animals perceive guidance cues, including polarity, intensity, and inclination from the geomagnetic field, to navigate long distances (Mouritsen, 2018) and home ranges (Voss et al., 2007). In these models and several recently proposed alternative hypotheses (Natan et al., 2020; Nimpf et al., 2019), a fundamental question is how biomolecules respond to changes in external magnetic fields. Metals and metalloproteins are certainly promising candidates for animal magnetoreception, as suggested by the magnetite, biocompass, and several alternative models.

Metal ions, even at low concentrations, play an important role throughout the biological clades in various biological processes, acting as catalysts, signaling agents and redox centers. Most metal ions bind to specific proteins or enzymes, called metal-binding proteins and metalloproteins, which account for around 40% of all enzymes with known 3D structures in the Protein Data Bank (PDB) and nearly half of all naturally occurring proteins in biology (Garcia et al., 2006; Liu et al., 2014; Waldron et al., 2009). Iron-sulfur proteins, among the most ancient metalloproteins on Earth, serve as electron carriers in all kingdoms of life due to the redox properties of iron-sulfur clusters (Johnson et al., 2005; Kiley & Beinert, 2003; Lill, 2009).

While iron-sulfur proteins are well known for their critical roles of electron transport (ET) in fundamental physiological processes such as photosynthesis and cellular respiration, they are also involved in nitrogen fixation and DNA replication and repair (Fontecave, 2006; Johnson et al., 2005; Kiley & Beinert, 2003; Mettert & Kiley, 2015; Rouault, 2015). However, novel functions of this ancient protein superfamily continue to be discovered. As a highly conserved A-type iron-sulfur protein originally identified as a scaffolding protein for iron-sulfur cluster assembly (Jacobson et al., 1989; Ollagnier-De-Choudens et al., 2001), IscA has also been proposed as a novel magnetoreceptor in animals, thus renamed MagR (Qin et al., 2016). Recent studies have reported the conserved interaction between MagR and Cry in almost all animal species, the colocalization of MagR and Cry4 proteins in pigeon retina, and the intrinsic magnetic properties of the MagR/Cry complex, leading to the development of the MagR/Cry-based biocompass model of animal magnetoreception (Lohmann, 2016; Qin et al., 2016).

Various theoretical approaches have been applied to explain how the MagR/Cry complex senses the geomagnetic field, with the biocompass model further modified and expanded to quantum mechanics in the past few years (Cao & Yan, 2018; Xiao et al., 2020; Xie, 2022; Zhao et al., 2022). In the latest view of the biocompass model, magnetically responsive MagR and photosensitive Cry form a rod-like complex with intrinsic magnetic properties (Qin et al., 2016). An evolutionally conserved intermolecular electron transport (ET) pathway connects MagR and Cry in the complex, in which electrons travel stepwise along a flavin-tryptophan chain, as described in the classic radical pair model and further extended to iron-sulfur clusters in MagR (Xie, 2022). Therefore, the MagR/Cry-based biocompass model may provide a solution for inclination and polarity detection and help illuminate the mechanism of light- and magneto-coupling and crosstalk between magnetoreception and circadian rhythm behavior in animals.

Despite rapid and significant progress in elucidating the underlying mechanisms of MagR and the MagR/Cry-based biocompass model, questions related to the origin of magnetism in MagR and the MagR/Cry complex remain unresolved. Therefore, the metal-binding properties of MagR and their effects on protein magnetism have attracted attention. The iron-sulfur cluster binding of MagR (IscA) was first identified in *Escherichia coli* IscA (ecIscA) (Ollagnier-De-Choudens et al., 2001). Several studies have further revealed that *E. coli* IscA exhibits unique and robust iron-binding activity, indicating that IscA may act as an iron chaperone for iron-sulfur cluster biogenesis (Ding & Clark, 2004; Landry et al., 2013; Yang et al., 2015). Mononuclear iron-bound MagRs (IscAs) have also been identified in yeast and humans, playing roles in the *de novo* synthesis of [4Fe-4S] clusters in mitochondria (Lill et al., 2012; Lu et al., 2010; Muhlenhoff et al., 2011). However, whether MagR simultaneously binds iron and iron-sulfur clusters in eukaryotic organisms, and how iron binding and iron-sulfur binding confer protein magnetism and animal magnetoreception, remains unclear.

Therefore, the characterization of iron-sulfur clusters and mononuclear iron bound to MagR will certainly shed light on these questions. Two forms of iron-sulfur clusters, i.e., [2Fe-2S] and [3Fe-4S], have been identified in pigeons (*Columba livia*) MagR (clMagR) and different iron-sulfur clusters bound to clMagR show different magnetic properties, suggesting a possible magnetic switch of MagR via iron-sulfur cluster binding (Guo et al., 2021). Based on the self-assembly dynamics of clMagR, tetramer is considered as a building block for hierarchical assembly (Yang et al., 2022). Another recent study using small-angle X-ray scattering (SAXS) suggested that clMagR assembly is controlled by the external static magnetic field, in which iron-sulfur cluster binding is thought to be critical (Arai et al., 2022).

Taken together, these data suggest that metal binding, including iron binding and iron-sulfur cluster binding, may not only play a role in magnetism but also in the magnetic response of MagR. Therefore, it is important to verify whether pigeon MagR binds mononuclear iron as well as iron-sulfur clusters and how iron and iron-sulfur clusters contribute to the magnetic properties of MagR.

Here, the iron-binding activity of clMagR was confirmed by spectroscopy and site-directed mutagenesis. Interestingly, both iron- and iron-sulfur-binding contributed essentially and indispensably to the magnetic properties of clMagR at temperatures of 5 K and 300 K. Mutating either one turned the

protein from paramagnetic to diamagnetic. Our results suggest that iron- and iron-sulfur-binding of MagR may be species-specific and work synergistically with protein magnetism. This study should provide insights into the huge diversity of magnetoreception in different organisms.

MATERIALS AND METHODS

Protein expression and purification

The expression vector containing the pigeon (*Columba livia*) *MagR* (*clMagR*) gene was constructed as described previously (Qin et al., 2016), and the *clMagR*^{Y65A} and *clMagR*^{Y65F} plasmids were obtained by site-directed mutagenesis (Tiangen Inc., China) according to the manufacturer's instructions. Wild-type clMagR and mutant proteins were recombinantly expressed in the *E. coli* strain BL21 (DE3). Bacterial cells were harvested after induction with 20 μmol/L isopropyl-D-1-thiogalactopyranoside (IPTG) overnight at 15 °C. The harvested bacterial cells were resuspended in lysis buffer (20 mmol/L Tris, 500 mmol/L NaCl, pH 8.0) with complete protease inhibitor cocktail and lysed by sonication on ice. After centrifugation at 4 °C and 15 000 r/min for 30 min, the supernatant was collected and loaded into a Strep-Tactin affinity column (IBA GmbH, Germany). The column was washed with 20 column volumes (CV) of washing buffer (20 mmol/L Tris, 500 mmol/L NaCl, pH 8.0) to remove unbound proteins. After washing, clMagR and its mutants were eluted using elution buffer (20 mmol/L Tris, 500 mmol/L NaCl, 5 mmol/L desthiobiotin, pH 8.0). For sodium dodecyl-sulfate polyacrylamide gel electrophoresis (SDS-PAGE), a protein ladder (Thermo Scientific, Product# 26616, USA) was used as the molecular weight standard.

Electron paramagnetic resonance (EPR) measurement

The EPR spectra of the clMagR samples were recorded at the X-band on a Bruker EMX plus 10/12 spectrometer using an Oxford ESR-910 liquid helium cryostat. Briefly, 200 μL of 1 mmol/L purified protein (oxidized) was mixed with 50 μL of glycerol in TBS buffer (20 mmol/L Tris, 150 mmol/L NaCl, pH 8.0). The reduced proteins were prepared by adding 10 mmol/L $Na_2S_2O_4$ to the samples. The protein samples were transferred into a quartz EPR tube (Wilmad 707-SQ-250 M) and frozen in liquid nitrogen. The EPR signals were monitored at different temperatures (10 K, 25 K, 45 K, and 60 K) with a microwave frequency of 9.40 GHz, microwave power of 2 mW, modulation amplitude of 2.0 G, and receive gain of 1.0×10^4.

Ultraviolet-visible absorption and circular dichroism measurement

Ultraviolet-visible (UV-Vis) spectra were scanned at room temperature at near UV-visible wavelengths (300–600 nm) and using a NanoDrop spectrophotometer (NanoDrop OneC, Thermo Scientific, USA). Circular dichroism (CD) spectroscopy was used to monitor protein-bound co-factors, such as metals or iron-sulfur clusters, in the near UV-visible range (300–600 nm). Wild-type clMagR and mutant proteins (100 μmol/L or 300 μmol/L when L-cysteine was added) were measured using a MOS-500 (Biologic) CD spectrometer at room temperature. Phosphate-buffered saline (PBS) buffer (0.01 mol/L, NaCl, $Na_2HPO_4\cdot12H_2O$, $NaH_2PO_4\cdot2H_2O$, pH 7.4) was used as a blank control.

Ferrozine assay

The ferrozine assay is an accurate and rapid method of iron quantitation in biological systems (De Mello Gabriel et al., 2021; Im et al., 2013). Here, a series of ferric chloride ($FeCl_3$) solutions (0.1–1.0 mmol/L) were prepared in HCl (1 mol/L) to generate a standard curve. Iron content in MagR and its mutant proteins was quantified and analyzed using the ferrozine assay based on the stand curve. Briefly, 80 μL of HAHCl (hydroxylamine hydrochloride, 10% w/v HAHCl in 1 mol/L HCl) was mixed with 20 μL of protein (0.1 mmol/L). After incubating the mixture at 37 °C for 30 min in the dark, 100 μL of ferrozine solution (1 g/L ferrozine in 50% w/v ammonium acetate) was added to each well and incubated at 37 °C for 5 min in the dark. The iron-ferrozine complex was measured at 562 nm on a microplate reader (Tecan Spark). Iron levels in the protein samples were determined by linear regression analysis. There were three replicates for each protein sample. Histograms and statistical analyses were performed using GraphPad Prism software. Protein samples were tested for differences in total iron using a *t*-test and were considered significantly different at $P<0.05$.

Chemical reconstitution of iron-sulfur clusters in clMagR^{WT} and mutants

The purified wild-type clMagR and mutant proteins (400 μmol/L) were incubated with 10 mmol/L $Na_2S_2O_4$ and 10 mmol/L ethylenediaminetetraacetic acid (EDTA) overnight at 4 °C in TBS buffer (20 mmol/L Tris, 150 mmol/L NaCl, pH 8.0) to remove iron-sulfur clusters. The mixture was desalted using a PD MiniTrap G-25 desalting column (GE Healthcare, USA). The obtained protein samples were labeled as "apo-clMagR". Apo-clMagR was incubated with 5 mmol/L dithiothreitol (DTT) for 30 min at 4 °C, then with $Fe(NH_4)_2(SO_4)_2$ (1.6 mmol/L) and Na_2S (1.6 mmol/L) overnight at 4 °C. The mixture was desalted using a PD MiniTrap G-25 desalting column (GE Healthcare, USA) and the obtained protein samples were labeled as "chem re clMagR".

Iron reconstitution in clMagR^{WT} and mutants

The purified wild-type clMagR and mutant proteins (100 μmol/L) were incubated with the indicated concentrations of $Fe(NH_4)_2(SO_4)_2$ (0–100 μmol/L) in the presence of DTT (2 mmol/L) at room temperature for 30 min, followed by protein repurification with a PD MiniTrap G-25 desalting column (GE Healthcare, USA). The absorption peak at 315 nm represents iron binding in clMagR.

Iron-sulfur cluster transfer experiments

The purified IscU protein (400 μmol/L) was incubated with $Fe(NH_4)_2(SO_4)_2$ (3.2 mmol/L) and Na_2S (3.2 mmol/L) in the presence of DTT (5 mmol/L) for 3–4 h at room temperature. The mixture was desalted using a PD MiniTrap G-25 desalting column (GE Healthcare, USA). The obtained proteins were labeled as "holo-IscU". For the *in vitro* iron-sulfur cluster transfer experiments, holo-IscU was incubated with Strep-tagged apo-clMagR in the presence of DTT (5 mmol/L) for 2–3 h. The two proteins were separated using a Strep-Tactin

affinity column (IBA) after reaction. Iron-sulfur cluster transfer was monitored by UV-Vis absorption at 315 nm and 420 nm.

Iron transfer experiments

Purified IscU (100 μmol/L) was incubated with clMagR (Strep-tagged, as purified, 150 μmol/L), DTT (2 mmol/L), L-cysteine (1 mmol/L), and IscS (1 μmol/L) at 4 °C for 3–4 h. After incubation, the two proteins were separated using a Strep-Tactin affinity column (IBA). Iron transfer was monitored by UV-Vis absorption at 315 nm and 415 nm.

Magnetic measurement

The magnetic moment of the proteins was measured using a superconducting quantum interference device (SQUID) magnetometer. Briefly, protein samples, including wild-type clMagR and mutants (in TBS buffer containing 20 mmol/L Tris, 150 mmol/L NaCl, pH 8.0) and blank controls (20 mmol/L Tris, 150 mmol/L NaCl, pH 8.0), were lyophilized using a freeze dryer (Heto PowerDry LL3000, Thermo Scientific, USA). An MPMS-3 magnetometer (Quantum Design, USA) equipped with a SQUID sensor was used for magnetic measurement of the lyophilized samples at different temperatures (5 K and 300 K). The fields applied were between −2 and 2 T. MH curves (magnetization (M) curves measured versus applied fields (H)) of proteins were obtained after subtracted the background from the buffer control.

RESULTS

Iron-binding activity of pigeon MagR and bacterial IscA

MagR/IscA is an evolutionarily conserved A-type protein that plays essential roles in iron-sulfur cluster assembly and animal magnetoreception (Lu et al., 2020; Qin et al., 2016). However, the iron-binding and iron-sulfur-binding activities of this protein are complex and vary from species to species (Ding & Clark, 2004; Guo et al., 2021; Landry et al., 2013; Lill et al., 2012; Lu et al., 2010; Muhlenhoff et al., 2011; Yang et al., 2015). The IscA homodimer can bind [2Fe-2S] and [4Fe-4S] through three conserved cysteine residues (C35, C99, and C101 for *E. coli*) (Krebs et al., 2001; Ollagnier-De-Choudens et al., 2001), and iron-sulfur cluster-binding patterns have been revealed by the three-dimensional (3D) structure of [2Fe-2S]-bound IscA from *Thermosynechococcus elongatus* (Morimoto et al., 2006). Tight ferric iron-binding activity (Kd, 3×10^{19} M^{-1}) of IscA from *E. coli* and humans (*Homo sapiens*) has been reported and a conserved residue (Y40) for *E. coli* has been identified as a potential site involved in iron binding (Ding & Clark, 2004; Lu et al., 2010). As an avian homologous protein of IscA, [2Fe-2S] and [3Fe-4S] cluster binding via three conserved cysteine residues (C60, C124 and C126) has been confirmed in pigeon MagR (Guo et al., 2021).

To further investigate whether pigeon MagR can bind mononuclear iron, in addition to known iron-sulfur cluster binding, sequence alignment of MagR/IscA from seven representative species was performed (Figure 1A). The putative iron-binding site tyrosine 65 (Y65 in pigeon MagR, corresponding to Y40 in *E. coli* IscA) is evolutionarily conserved (Ding & Clark, 2004; Lu et al., 2010). Both proteins, i.e., clMagR from pigeon and ecIscA from *E. coli*, were recombinantly expressed and purified to homogeneity under aerobic conditions. Total iron content in clMagR and ecIscA was measured using the ferrozine assay (Figure 1B) after the addition of L-cysteine (Im et al., 2013; Jeitner, 2014). Iron-sulfur binding was confirmed by UV-Vis absorption spectra (Figure 1C). Pigeon MagR showed significantly higher total iron content and iron-sulfur cluster binding compared to the bacterial IscA protein. Interestingly, ecIscA showed an extremely low absorption peak at 415 nm and undetectable absorption at 456 nm, indicating very low or no iron-sulfur cluster binding in the purified protein, consistent with previous reports (Ding & Clark, 2004; Landry et al., 2013).

Y65 mutation decreased total iron-content in pigeon MagR

A 3D homology model of clMagR was obtained as described previously (Qin et al., 2016; Xie, 2022), showing that the putative iron-binding site Y65 was distant from the iron-sulfur cluster-binding site formed by C60, C124, and C126 (Figure 1D, E). The distinctive binding sites allowed us to mutate the iron-binding site but preserve iron-sulfur binding. Therefore, two mutants (clMagR^{Y65F} and clMagR^{Y65A}) were generated in which the conserved tyrosine 65 (Y65) was substituted with phenylalanine (Y65F) or alanine (Y65A), respectively. Both mutants were used to test iron-binding activity, and clMagR^{3M} was obtained by mutating three conserved cysteine residues (C60/C124/C126) to alanine to abolish the iron-sulfur cluster binding of clMagR (Figure 2).

Wild-type clMagR and three mutants (clMagR^{Y65F}, clMagR^{Y65A}, and clMagR^{3M}) were freshly prepared and purified to homogeneity under aerobic conditions (Figure 2A). The UV-Vis spectra showed absorption peaks in the 300–600 nm region. As shown in Figure 2A, clMagR^{WT} and two Y65 mutants (clMagR^{Y65F} and clMagR^{Y65A}) showed absorption peaks at 315 and 415 nm, and a shoulder at 456 nm, indicating correct iron-sulfur cluster incorporation in the protein. However, absorption decreased overall in clMagR^{Y65F} and clMagR^{Y65A}, likely because Y65-mediated iron binding of the protein was damaged and/or iron-sulfur cluster binding was affected by allosteric regulation. Purified clMagR^{3M} showed abolished absorption, suggesting that the three conserved cysteines are required for both iron binding and iron-sulfur binding.

CD spectroscopy was applied to characterize the iron-sulfur cluster types and their protein environments. As shown in Figure 2B, clMagR^{WT} and two Y65 mutants, but not clMagR^{3M}, showed distinct positive peaks at 371 nm and 426 nm and three negative peaks at 324 nm, 396 nm, and 463 nm, respectively, suggesting that iron-sulfur cluster (especially [2Fe–2S]) binding was preserved in clMagR^{Y65F} and clMagR^{Y65A}. Iron-sulfur cluster binding and iron-sulfur cluster types in clMagR^{WT} and the two Y65 mutants were further confirmed by EPR spectroscopy (Supplementary Figure S1).

As L-cysteine can efficiently release iron from bacterial IscA (Ding et al., 2005; Landry et al., 2013), we tested whether iron can also be extruded from pigeon MagR by adding L-cysteine to a purified clMagR^{WT} protein solution. UV-Vis absorption of clMagR showed a gradual decrease and final disappearance after 2 h of incubation, indicating that iron was extruded from

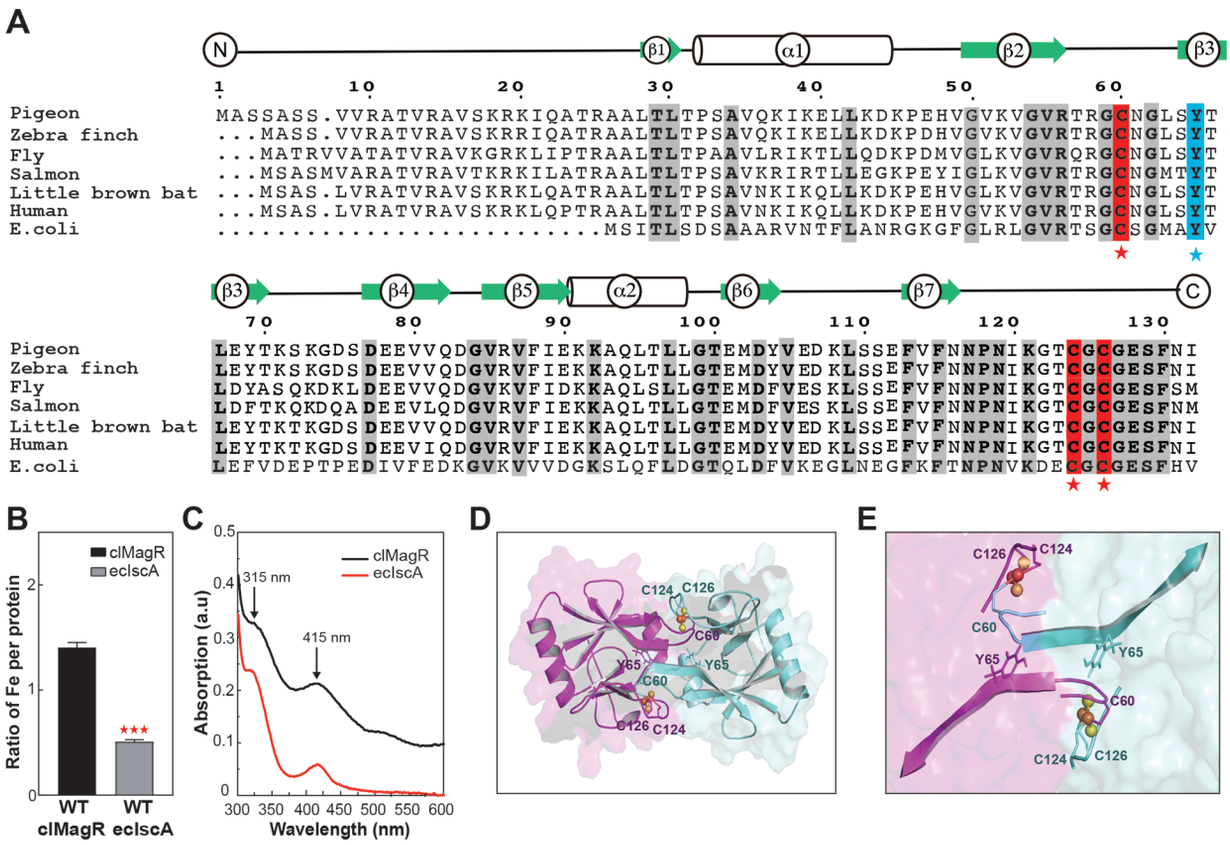

Figure 1 Iron binding in clMagR and IscA

A: Sequence alignment of MagR in seven representative species. Predicted secondary structures are shown on upper line, with two alpha-helices (represented by cylinders) and seven beta-strands (represented by arrows). Conserved residues with iron-sulfur cluster-binding properties are shown with red background, indicated by stars. B: Total iron content of purified clMagR and ecIscA measured by ferrozine assay as the ratio of iron atoms per protein monomer. *T*-tests were used to test for differences between repeated measures, and $P<0.05$ was considered significantly different. C: UV-Vis absorption spectra of clMagR and IscA. D: Structural model showing putative iron-binding site (Y65) and iron-sulfur cluster-binding site (C60, C124, and C126), in which two conserved cysteine residues (C124 and C126) of one monomer and one cysteine (C60) of a second monomer form a complete cluster-binding site. E: Close view of iron-binding site and iron-sulfur cluster-binding site.

both iron-center and iron-sulfur clusters in clMagR (Figure 2C). Iron release was also confirmed by CD spectroscopy (Figure 2D). As the [4Fe–4S] and [3Fe–4S] clusters usually exhibit negligible CD intensity compared to [2Fe–2S] (Mapolelo et al., 2012), to validate whether L-cysteine can also extrude iron from [3Fe–4S], EPR spectroscopy at 10 K was applied to monitor iron-release from oxidized clMagR upon L-cysteine incubation (10 min to 2 h). As shown in Figure 2E, the rhombic EPR signals at g=2.016, g=2.004, and g=1.998 indicated the presence of [3Fe-4S] in clMagR before L-cysteine incubation. The signals gradually decreased and nearly disappeared after 2 h, suggesting that iron was extruded from [3Fe–4S] clusters by L-cysteine through ligand exchange (Im et al., 2013; Jeitner, 2014). Therefore, the total iron content measured using the ferrozine assay after the addition of L-cysteine contained all iron released from the protein, including iron from the iron-binding and iron-sulfur-binding sites (e.g., iron from both [2Fe–2S] and [3Fe–4S] clusters).

Purified wild-type clMagR and three mutants (clMagR^{Y65F}, clMagR^{Y65A}, and clMagR^{3M}) showed different coloration at the same concentration (300 μmol/L, Figure 2F). The clMagR^{WT} protein was dark brown in solution, whereas clMagR^{Y65A} was yellowish and clMagR^{Y65F} was brown, in contrast to the colorless clMagR^{3M} protein. The ferrozine assay of all four proteins after L-cysteine incubation confirmed that clMagR^{WT} contained the highest total iron content, while the Y65 mutants (clMagR^{Y65F} and clMagR^{Y65A}) and three cysteine mutation (clMagR^{3M}) all showed significantly decreased iron content (Figure 2F). The iron content of clMagR^{3M} was nearly abolished, probably due to the loss of iron-sulfur cluster binding and diminished iron binding. The mutagenesis data suggested that Y65 was involved in iron-binding activity, and the three conserved cysteines were required for high-affinity iron binding.

Iron binding is mediated by Y65 in pigeon MagR

EPR measurement was applied to identify iron-sulfur cluster binding and directly validate iron binding in the proteins. As shown in Figure 3A, wild-type clMagR displayed a signal at g=4.3, which is a distinctive peak reflecting a mononuclear ferric iron center in the protein. In contrast, this peak disappeared in the EPR spectra of clMagR^{Y65A}, clMagR^{Y65F},

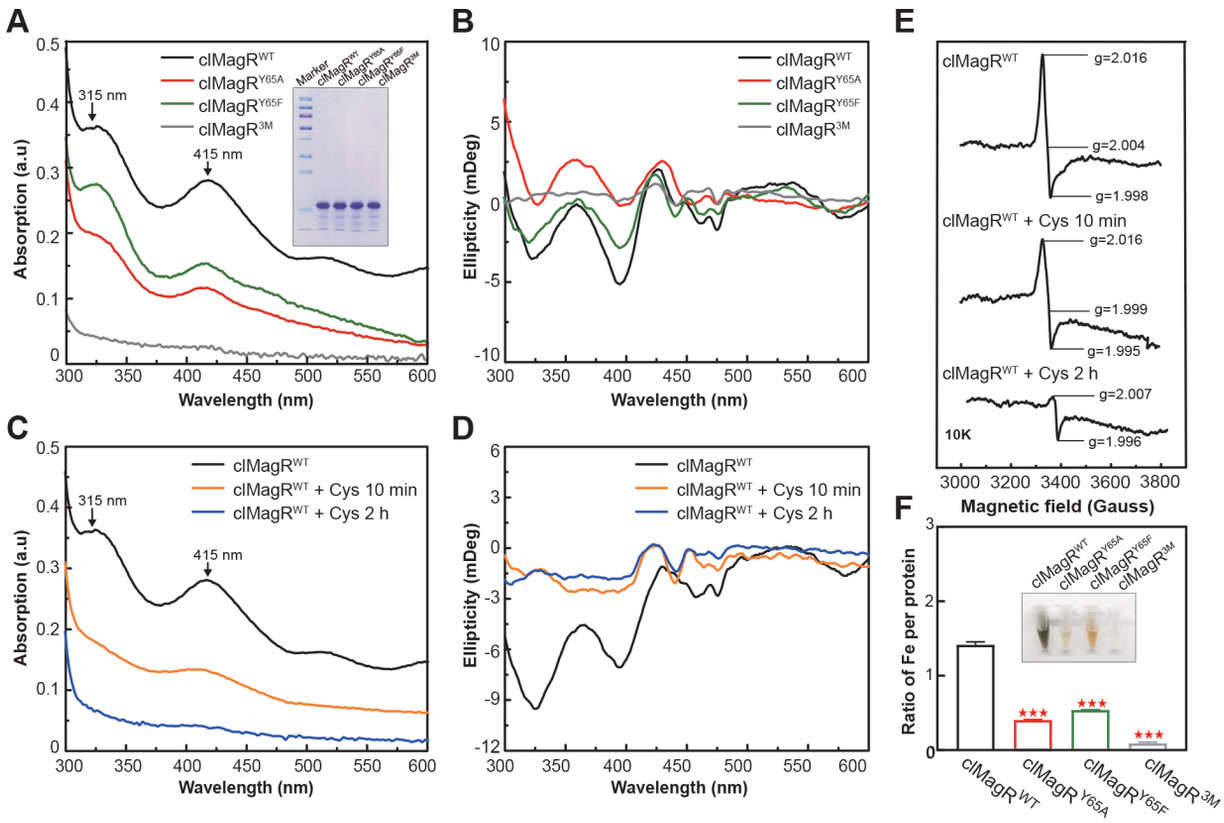

Figure 2 Y65 mutation decreased iron content but preserved iron-sulfur binding in pigeon MagR

A: UV-Vis absorption spectra of clMagR^{WT} (black), clMagR^{Y65A} (red), clMagR^{Y65F} (green), and clMagR^{3M} (gray). SDS-PAGE of purified protein is shown as inset. B: CD spectra of clMagR^{WT} (black), clMagR^{Y65A} (red), clMagR^{Y65F} (green), and clMagR^{3M} (gray). C: UV-Vis absorption spectra of clMagR^{WT} after incubation with L-cysteine at 4 °C for various time points. D: CD spectra of clMagR^{WT} after incubation with L-cysteine at 4 °C for various time points. E: EPR spectra of clMagR recorded at 10 K, after incubation with L-cysteine at 4 °C for various time points. F: Total iron content of purified wild-type clMagR and mutants measured by ferrozine assay as the ratio of iron atoms per protein monomer. *T*-tests were used to test for differences between repeated measures, and $P<0.05$ was considered significantly different.

and clMagR^{3M} (Figure 3A), suggesting that the ferric iron center was abolished by Y65 mutation, as well as by the three conserved cysteine mutations.

Iron reconstitution experiments were also performed with wild-type clMagR and two Y65 mutants to investigate whether Y65 mutation disrupts iron-binding capacity *in vitro*. Briefly, proteins were incubated with increasing concentrations of ferrous iron, then repurified based on previously described procedures (Ding et al., 2005; Landry et al., 2013). As shown in Figure 3, in both clMagR^{Y65A} (Figure 3D, E) and clMagR^{Y65F} (Figure 3F, G), the absorption peak at 315 nm, which represents iron binding of the protein, only showed a slight increase after incubation with ferrous iron in the presence of DTT. In contrast, clMagR^{WT} showed a significant increase in the absorption peak at 315 nm after iron reconstitution (Figure 3B, C). Among the three proteins, clMagR^{Y65A} showed saturated absorption at a very low concentration and nearly no increase upon iron reconstitution, indicating that iron-binding activity was abolished in this mutant. Therefore, based on these findings, we concluded that Y65 directly mediated iron binding, and mutating Y65 diminished or abolished iron-binding activity in pigeon MagR.

As iron binding in clMagR is very stable, we next tested whether iron-loaded clMagR can serve as an iron donor to provide iron for iron-sulfur cluster assembly in IscU *in vitro*. The iron transfer mechanism of ecIscA has been explored previously, showing that both L-cysteine and cysteine desulfurase (IscS) are required for the process (Ding et al., 2005). As shown in Figure 4, when iron-loaded clMagR^{WT} and apo-IscU were incubated with L-cysteine and IscS anaerobically at 37 °C for 30 min, absorption of iron-loaded clMagR^{WT} gradually disappeared (Figure 4A), with the concurrent appearance and gradual increase in absorption of iron-sulfur cluster binding in repurified IscU (Figure 4B). However, as clMagR^{Y65A} and clMagR^{Y65F} showed reduced or no iron binding, almost no change (clMagR^{Y65A}, Figure 4C) and a minor decrease (clMagR^{Y65F}, Figure 4E) in UV-Vis absorption were observed in this process. Correspondingly, as IscU could not obtain much iron from clMagR^{Y65A} or clMagR^{Y65F}, only a minor UV-Vis absorption increase was observed after incubation with the two Y65 mutants (Figure 4D, F).

Taken together, we concluded that pigeon MagR exhibited both iron binding and iron-sulfur cluster binding, and iron binding was mediated by conserved Y65, with the potential involvement of three conserved cysteines (C60, C124, and

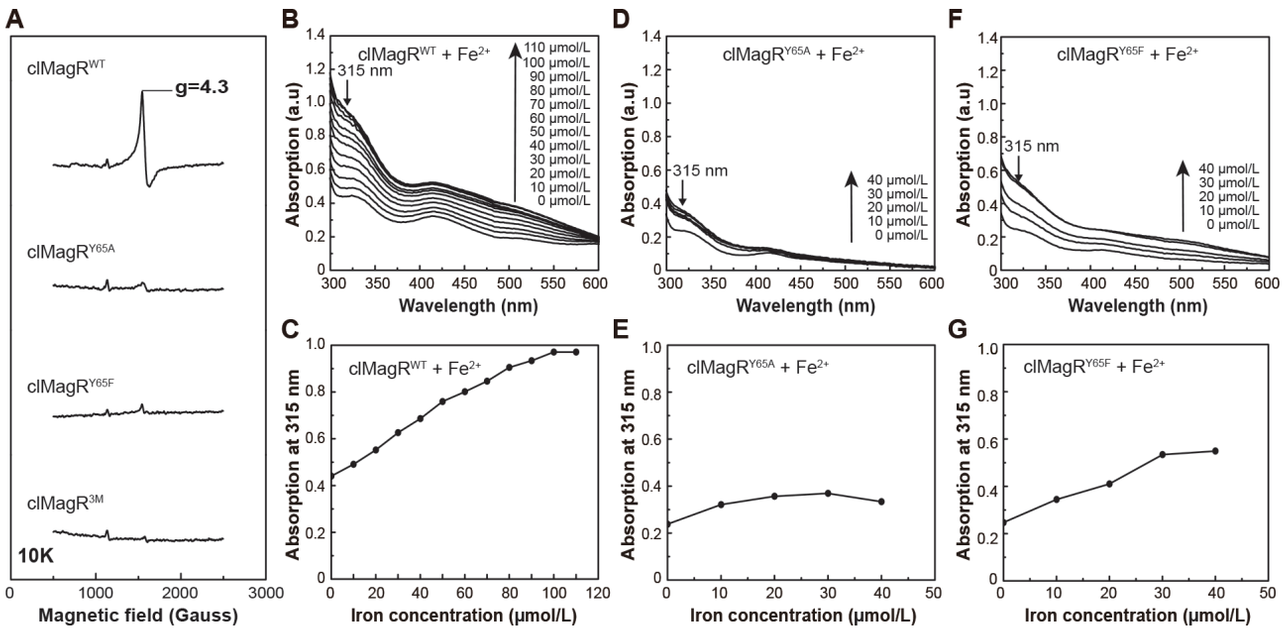

Figure 3 Iron binding in pigeon MagR was mediated by Y65

A: EPR spectra of wild-type clMagR and mutants recorded at 10 K to validate ferric iron binding in protein. B, D, F: UV-Vis absorption spectra of clMagR^{WT} (B), clMagR^{Y65A} (D), and clMagR^{Y65F} (F) after iron-reconstitution. Purified proteins were incubated with various concentrations of $Fe(NH_4)_2(SO_4)_2$ in presence of DTT (2 mmol/L) at 4 °C for 20 min, followed by repurification of protein, with iron binding of different proteins monitored by UV-Vis absorption spectroscopy. C, E, G: Iron binding curves of clMagR^{WT} (C), clMagR^{Y65A} (E), and clMagR^{Y65F} (G). Amplitude of absorption peak at 315 nm for different proteins were obtained from the spectra of B, D, and F, respectively, and plotted as a line graph.

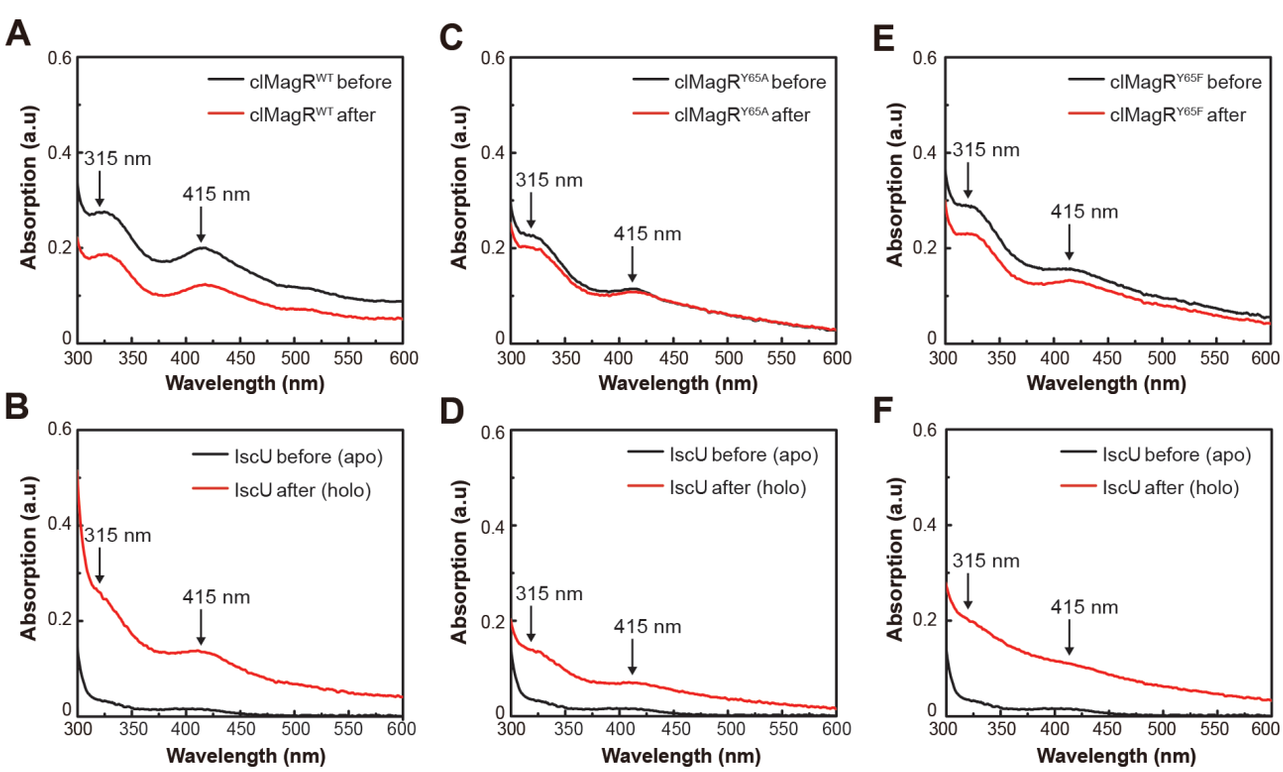

Figure 4 Iron transfer from wild-type clMagR and mutants to IscU in presence of L-cysteine and IscS

clMagR^{WT}, clMagR^{Y65A}, and clMagR^{Y65F} were incubated anaerobically with apo-IscU in the presence of L-cysteine and IscS. UV-Vis absorption spectra of clMagR^{WT} and repurified IscU (A and B, respectively), clMagR^{Y65A} and repurified IscU (C and D, respectively), and clMagR^{Y65F} repurified IscU (E and F, respectively) are shown as before (black lines) and after (red lines) incubation.

C126).

Iron-sulfur binding is independent of mononuclear iron binding in pigeon MagR

As mentioned above, both clMagR^{Y65F} and clMagR^{Y65A} retained iron-sulfur cluster binding. To further investigate the connection between iron binding and iron-sulfur binding in pigeon MagR, iron-sulfur cluster reconstitution was performed on the clMagR^{WT}, clMagR^{Y65A}, and clMagR^{Y65F} proteins, as described previously (Guo et al., 2021). In brief, freshly purified proteins were incubated with $Na_2S_2O_4$ and EDTA, followed by desalting to completely remove the iron-sulfur clusters and obtain apoproteins (solid lines, Figure 5A–C). The iron-sulfur apoproteins were then provided with iron and sulfide under reducing conditions to spontaneously form iron-sulfur clusters (dotted lines, Figure 5A–C). Iron-sulfur cluster assembly was monitored and verified using UV-Vis spectral analysis (Figure 5A–C). EPR spectroscopy was applied to confirm the incorporation of iron-sulfur clusters in the chemically reconstituted clMagR^{WT}, clMagR^{Y65A}, and clMagR^{Y65F} proteins (Figure 5D–F). Results showed that we successfully reconstituted iron-sulfur clusters into the clMagR^{WT}, clMagR^{Y65A}, and clMagR^{Y65F} proteins using this approach, and that Y65 mutation did not affect the iron-sulfur-binding activity of clMagR.

Consistently, the Y65 mutation in clMagR did not affect iron-sulfur cluster transfer from IscU *in vitro*. Wild-type clMagR and two Y65 mutants were incubated anaerobically with holo-IscU. The UV-Vis absorption spectra of repurified IscU and clMagR^{WT}, clMagR^{Y65A}, and clMagR^{Y65F} clearly demonstrated that iron-sulfur clusters were successfully transferred from holo-IscU to clMagR and mutants (Supplementary Figure S2), suggesting that iron-sulfur cluster-binding activity was fully preserved in the Y65 mutants, and iron-sulfur binding appears to be independent of mononuclear iron binding.

Iron- and iron-sulfur-binding play essential and indispensable roles in the magnetic properties of MagR

For the first time, we unambiguously showed that pigeon MagR possesses both iron binding and iron-sulfur binding simultaneously, raising several important questions about the origin of the magnetic moment of MagR in pigeons and other avian species. Notably, do iron and iron-sulfur clusters both contribute to the magnetic properties of this protein? How do iron and iron-sulfur clusters coordinate the magnetic response of MagR to external magnetic field changes during navigation?

To address these questions, we measured the magnetic moment of wild-type clMagR and two mutants (clMagR^{Y65A} and clMagR^{3M}) using SQUID magnetometry. This is an effective and sensitive way to measure magnetic properties, especially extremely subtle magnetic fields, and one of the few practical and feasible ways to characterize biological samples with extremely low magnetic moments.

Magnetic measurements were performed at different temperatures (5 K and 300 K) and MH curves were generated to compare the magnetic susceptibility of the three different proteins. It is worth noting that, according to our results, wild-type pigeon MagR contains both mononuclear iron binding and iron-sulfur cluster binding, whereas clMagR^{Y65A} only shows iron-sulfur cluster binding and clMagR^{3M} displays neither.

The iron- and iron-sulfur-bound wild-type clMagR was

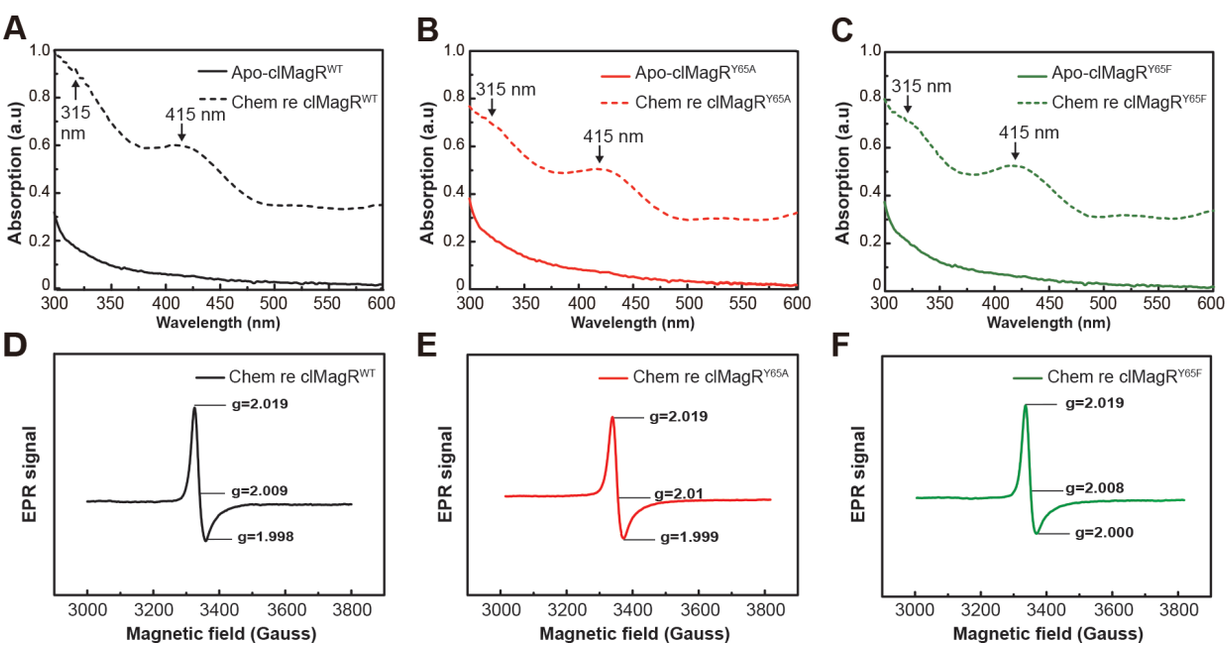

Figure 5 Y65 mutation does not affect iron-sulfur binding in clMagR

A–C: Chemical reconstitution-mediated iron-sulfur cluster assembly on apo-clMagR^{WT} (A), apo-clMagR^{Y65A} (B), and apo-clMagR^{Y65F} (C) monitored by UV-Vis absorption. UV-Vis spectra of apoproteins are shown as solid lines and chemically reconstituted proteins are shown as dotted lines. D–F: X-band EPR spectra of chemically reconstituted clMagR^{WT} (D), clMagR^{Y65A} (E), and clMagR^{Y65F} (F), showing iron-sulfur cluster incorporation in proteins. Spectra were recorded at 10 K.

paramagnetic at both 5 K and 300 K (Figure 6A, B, black). This may be due to the synergistic effects of mononuclear iron and [2Fe–2S] and [3Fe–4S] mixture binding to the protein (Guo et al., 2021). The MH curve of clMagR^{3M} exhibited obvious diamagnetic properties at 300 K and a barely detectable magnetic moment at 5 K (Figure 6A, B, gray), consistent with previous research (Guo et al., 2021) and suggesting that both iron-sulfur clusters and mononuclear iron are essential for clMagR magnetism. Surprisingly, however, Y65A mutation in clMagR totally abolished the magnetic moment of clMagR and turned the protein diamagnetic (Figure 6A, B, red), suggesting that iron-sulfur clusters alone are insufficient to generate paramagnetism, and both iron binding and iron-sulfur cluster binding are indispensable for pigeon MagR magnetism. These findings strongly suggest a possible synergistic mechanism of the MagR magnetism based on the concurrent iron-binding and iron-sulfur-binding features, which deserve further investigation and validation *in vivo*.

DISCUSSION

The recently proposed MagR/Cry-based biocompass model combines the concept of ferromagnetism (as in MagR/Cry combination) and the quantum compass mechanism (as in Cry). It offers a potential solution to how animals sense the geomagnetic field. However, several fundamental questions remain unresolved in this model. For example, what is the origin of the magnetic properties of MagR, which cannot be explained solely by the iron-sulfur clusters bound to the protein, as argued in previous research (Meister, 2016). As MagR (IscA) is a highly evolutionarily conserved protein, from bacteria to humans, how can such a conserved protein serve as a magnetoreceptor and be responsible for highly diverse migration and homing behaviors in the animal kingdom?

The data presented here may provide clues to these questions. Mononuclear iron-binding activity in iron-sulfur proteins has long been overlooked. Here, our study revealed tight iron-binding activity and concurrent iron-sulfur cluster-binding activity in the pigeon MagR, as well as their synergistic interactions. These results explain the significantly higher total iron content in pigeon MagR compared with other species, which may be an important feature of animal magnetoreception.

Among all iron-sulfur proteins, MagR is unique in many respects: it exhibits dynamic assembly and rod-like polymers and forms a stable complex with Cry in almost every species (Qin et al., 2016). It also demonstrates species-specific mononuclear iron binding and/or iron-sulfur cluster binding, as shown in our and previous studies (Ding & Clark, 2004; Landry et al., 2013; Lill et al., 2012; Lu et al., 2010; Muhlenhoff et al., 2011; Ollagnier-De-Choudens et al., 2001; Yang et al., 2015). Furthermore, the protein binds different iron-sulfur clusters, leading to different magnetic properties (Guo et al., 2021). It also shows self-assembly and hierarchical assembly features, and its assembly can be induced by external magnetic fields and modulated by iron-sulfur cluster binding (Arai et al., 2022; Yang et al., 2022). We demonstrated that both iron binding and iron-sulfur binding play essential and synergistic roles in MagR magnetism. These unique features enable MagR to achieve complex functions and diversity among species, even with highly conserved sequences.

It should be noted that the underlying mechanism of magnetism and magnetic response of MagR may be much more complex than previously thought. Light perception from Cry may modulate the magnetic properties of MagR in the complex. Possible electron transfer between MagR and Cry could connect the biocompass model and radical-pair model (Xie, 2022), allowing the protein machinery to serve as a biological quantum compass in animal magnetoreception and navigation. However, these scenarios are not optimal and tremendous potential remains for further exploration.

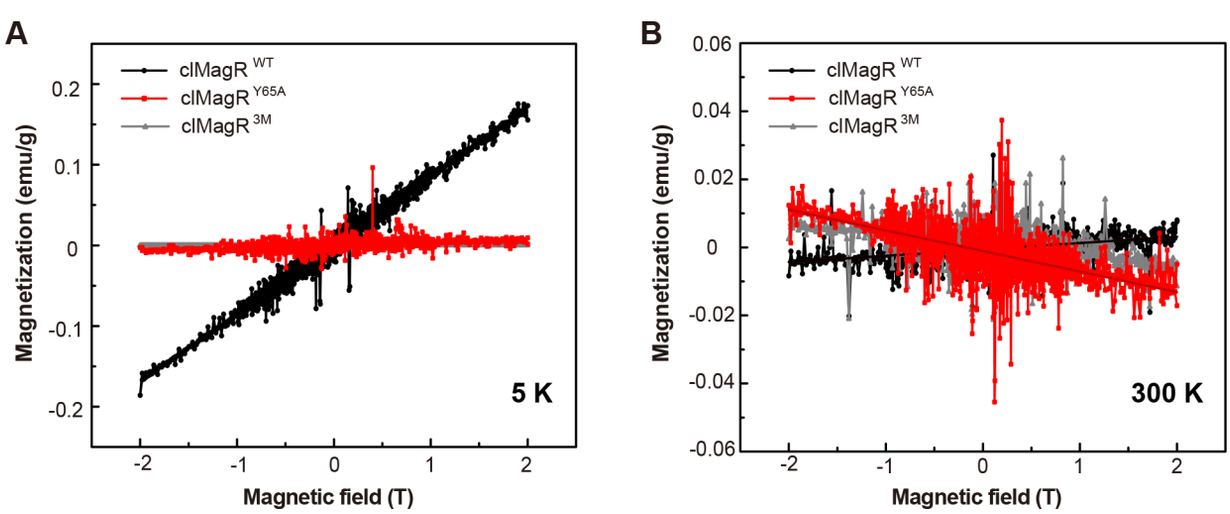

Figure 6 Both iron binding and iron-sulfur cluster binding are indispensable for magnetic properties of pigeon MagR

A: Field-dependent magnetization curves (MH) at 5 K for clMagR^{WT} (black), clMagR^{Y65A} (red), and clMagR^{3M} (gray). Mass magnetic susceptibilities in CGS unit were 8.53567e-6, 4.02513e-7, and 7.73049e-9 emu/g, respectively. B: Field-dependent magnetization curves (MH) at 300 K for clMagR^{WT} (black), clMagR^{Y65A} (red), and clMagR^{3M} (gray). Mass magnetic susceptibilities in CGS unit were 1.86982e-7, −6.0426e-7, and −2.86548e-7 emu/g, respectively.

SUPPLEMENTARY DATA

Supplementary data to this article can be found online.

COMPETING INTERESTS

The authors declare that they have no competing interests.

AUTHORS' CONTRIBUTIONS

C.X. conceived the idea and designed the study. Y.Z. carried out protein purification, site-directed mutagenesis, ferrozine assay, CD spectroscopy, and EPR experiments. Y.Z. and C.X. performed data analysis. P.Z and L.Z. helped with SQUID measurement and data analysis. T.T, M.W., P.Z., F.F., X.Z., Z.G., J.Z., H.X., L.Z., and S.W. provided valuable suggestions on data analysis. Y.Z. and C.X. wrote the paper. T.C., J.W., and X.Z. provided valuable discussions and edited the manuscript. All authors read and approved the final version of the manuscript.

ACKNOWLEDGMENTS

We are grateful to Prof. Huangen Ding from Louisiana State University (USA) for valuable discussions and inspiration to initiate this project. A portion of this work was performed at the Steady High Magnetic Field Facilities, High Magnetic Field Laboratory, CAS. We also thank Dr. Wei Tong and Jinxing Li for their technical support. We are grateful to the core facilities of the College of Life Sciences at the University of Science and Technology of China, and the core facilities of the College of Life Sciences at Anhui University for their help in CD spectral measurements. We also thank Dr. Jin Xiong from Carnegie Mellon University and Dr. Weiqiang Wang from Anhui University for very helpful discussions.

REFERENCES

Arai S, Shimizu R, Adachi M, Hirai M. 2022. Magnetic field effects on the structure and molecular behavior of pigeon iron–sulfur protein. *Protein Science*, **31**(6): e4313.

Cadiou H, McNaughton PA. 2010. Avian magnetite-based magnetoreception: a physiologist's perspective. *Journal of the Royal Society Interface*, **7 Suppl 2**(Suppl 2): S193–S205.

Cao YS, Yan P. 2018. Role of atomic spin-mechanical coupling in the problem of a magnetic biocompass. *Physical Review E*, **97**(4): 042409.

De Mello Gabriel GV, Pitombo LM, Rosa LMT, Navarrete AA, Botero WG, Do Carmo JB, et al. 2021. The environmental importance of iron speciation in soils: evaluation of classic methodologies. *Environmental Monitoring and Assessment*, **193**(2): 63.

Dennis TE, Rayner MJ, Walker MM. 2007. Evidence that pigeons orient to geomagnetic intensity during homing. *Proceedings of the Royal Society B:Biological Sciences*, **274**(1614): 1153−1158.

Ding BJ, Smith ES, Ding HG. 2005. Mobilization of the iron centre in IscA for the iron-sulphur cluster assembly in IscU. *Biochemical Journal*, **389**(Pt 3): 797–802.

Ding H, Clark RJ. 2004. Characterization of iron binding in IscA, an ancient iron-sulphur cluster assembly protein. *Biochemical Journal*, **379**(Pt 2): 433–440.

Fontecave M. 2006. Iron-sulfur clusters: ever-expanding roles. *Nature Chemical Biology*, **2**(4): 171−174.

Garcia JS, de Magalhães CS, Arruda MAZ. 2006. Trends in metal-binding and metalloprotein analysis. *Talanta*, **69**(1): 1−15.

Guo Z, Xu S, Chen X, Wang CH, Yang PL, Qin SY, et al. 2021. Modulation of MagR magnetic properties via iron–sulfur cluster binding. *Scientific Reports*, **11**(1): 23941.

Heyers D, Manns M, Luksch H, Güntürkün O, Mouritsen H. 2007. A visual pathway links brain structures active during magnetic compass orientation in migratory birds. *PLoS One*, **2**(9): e937.

Heyers D, Zapka M, Hoffmeister M, Wild JM, Mouritsen H. 2010. Magnetic field changes activate the trigeminal brainstem complex in a migratory bird. *Proceedings of the National Academy of Sciences of the United States of America*, **107**(20): 9394−9399.

Hore PJ, Mouritsen H. 2016. The radical-pair mechanism of magnetoreception. *Annual Review of Biophysics*, **45**: 299−344.

Im J, Lee J, Löffler FE. 2013. Interference of ferric ions with ferrous iron quantification using the ferrozine assay. *Journal of Microbiological Methods*, **95**(3): 366−367.

Jacobson MR, Brigle KE, Bennett LT, Setterquist RA, Wilson MS, Cash VL, et al. 1989. Physical and genetic map of the major nif gene cluster from Azotobacter vinelandii. *Journal of Bacteriology*, **171**(2): 1017−1027.

Jeitner TM. 2014. Optimized ferrozine-based assay for dissolved iron. *Analytical Biochemistry*, **454**: 36−37.

Johnsen S, Lohmann K. 2008. Magnetoreception in animals. *Physics Today*, **61**(3): 29−35.

Johnson DC, Dean DR, Smith AD, Johnson MK. 2005. Structure, function, and formation of biological iron-sulfur clusters. *Annual Review of Biochemistry*, **74**: 247−281.

Kiley PJ, Beinert H. 2003. The role of Fe–S proteins in sensing and regulation in bacteria. *Current Opinion in Microbiology*, **6**(2): 181−185.

Kirschvink JL, Walker MM, Diebel CE. 2001. Magnetite-based magnetoreception. *Current Opinion in Neurobiology*, **11**(4): 462−467.

Krebs C, Agar JN, Smith AD, Frazzon J, Dean DR, Huynh BH, et al. 2001. IscA, an alternate scaffold for Fe-S cluster biosynthesis. *Biochemistry*, **40**(46): 14069−14080.

Landry AP, Cheng ZS, Ding HG. 2013. Iron binding activity is essential for the function of IscA in iron-sulphur cluster biogenesis. *Dalton Transactions*, **42**(9): 3100−3106.

Lill R. 2009. Function and biogenesis of iron-sulphur proteins. *Nature*, **460**(7257): 831−838.

Lill R, Hoffmann B, Molik S, Pierik AJ, Rietzschel N, Stehling O, et al. 2012. The role of mitochondria in cellular iron-sulfur protein biogenesis and iron metabolism. *Biochimica et Biophysica Acta (BBA) – Molecular Cell Research*, **1823**(9): 1491−1508.

Liu J, Chakraborty S, Hosseinzadeh P, Yu Y, Tian SL, Petrik I, et al. 2014. Metalloproteins containing cytochrome, iron-sulfur, or copper redox centers. *Chemical Reviews*, **114**(8): 4366−4469.

Lohmann KJ. 2016. Protein complexes: a candidate magnetoreceptor. *Nature Materials*, **15**(2): 136−138.

Lu HM, Li JD, Zhang YD, Lu XL, Xu C, Huang Y, et al. 2020. The evolution history of Fe-S cluster A-type assembly protein reveals multiple gene duplication events and essential protein motifs. *Genome Biology and Evolution*, **12**(3): 160−173.

Lu JX, Bitoun JP, Tan GQ, Wang W, Min WG, Ding HG. 2010. Iron-binding activity of human iron-sulfur cluster assembly protein hIscA1. *Biochemical Journal*, **428**(1): 125−131.

Maeda K, Henbest KB, Cintolesi F, Kuprov I, Rodgers CT, Liddell PA, et al. 2008. Chemical compass model of avian magnetoreception. *Nature*, **453**(7193): 387−390.

Mapolelo DT, Zhang B, Naik SG, Huynh BH, Johnson MK. 2012. Spectroscopic and functional characterization of iron-sulfur cluster-bound forms of *Azotobacter vinelandii* ^{Nif}IscA. *Biochemistry*, **51**(41): 8071−8084.

Meister M. 2016. Physical limits to magnetogenetics. *eLife*, **5**: e17210.

Mettert EL, Kiley PJ. 2015. How is Fe-S cluster formation regulated?. *Annual Review of Microbiology*, **69**: 505−526.

Morimoto K, Yamashita E, Kondou Y, Lee SJ, Arisaka F, Tsukihara T, et al. 2006. The asymmetric IscA homodimer with an exposed [2Fe-2S] cluster suggests the structural basis of the Fe-S cluster biosynthetic scaffold. *Journal of Molecular Biology*, **360**(1): 117−132.

Mouritsen H. 2018. Long-distance navigation and magnetoreception in migratory animals. *Nature*, **558**(7708): 50−59.

Mühlenhoff U, Richter N, Pines O, Pierik AJ, Lill R. 2011. Specialized function of yeast Isa1 and Isa2 proteins in the maturation of mitochondrial [4Fe-4S] proteins. *Journal of Biological Chemistry*, **286**(48): 41205−41216.

Natan E, Fitak RR, Werber Y, Vortman Y. 2020. Symbiotic magnetic sensing: raising evidence and beyond. *Philosophical Transactions of the Royal Society B:Biological Sciences*, **375**(1808): 20190595.

Nimpf S, Nordmann GC, Kagerbauer D, Malkemper EP, Landler L, Papadaki-Anastasopoulou A, et al. 2019. A putative mechanism for magnetoreception by electromagnetic induction in the Pigeon Inner Ear. *Current Biology*, **29**(23): 4052−4059.e4.

Ollagnier-De-Choudens S, Mattioli T, Takahashi Y, Fontecave M. 2001. Iron-sulfur cluster assembly: characterization of IscA and evidence for a specific and functional complex with ferredoxin. *Journal of Biological Chemistry*, **276**(25): 22604−22607.

Qin SY, Yin H, Yang CL, Dou YF, Liu ZM, Zhang P, et al. 2016. A magnetic protein biocompass. *Nature Materials*, **15**(2): 217−226.

Ritz T, Adem S, Schulten K. 2000. A model for photoreceptor-based magnetoreception in birds. *Biophysical Journal*, **78**(2): 707−718.

Rodgers CT, Hore PJ. 2009. Chemical magnetoreception in birds: the radical pair mechanism. *Proceedings of the National Academy of Sciences of the United States of America*, **106**(2): 353−360.

Rouault TA. 2015. Mammalian iron-sulphur proteins: novel insights into biogenesis and function. *Nature Reviews Molecular Cell Biology*, **16**(1): 45−55.

Voss J, Keary N, Bischof HJ. 2007. The use of the geomagnetic field for short distance orientation in zebra finches. *NeuroReport*, **18**(10): 1053−1057.

Walcott C, Gould JL, Kirschvink JL. 1979. Pigeons have magnets. *Science*, **205**(4410): 1027−1029.

Waldron KJ, Rutherford JC, Ford D, Robinson NJ. 2009. Metalloproteins and metal sensing. *Nature*, **460**(7257): 823−830.

Wiltschko R, Wiltschko W. 1995. Magnetic Orientation in Animals. Berlin, Heidelberg: Springer.

Wiltschko W, Wiltschko R. 2005. Magnetic orientation and magnetoreception in birds and other animals. *Journal of Comparative Physiology A*, **191**(8): 675−693.

Xiao DW, Hu WH, Cai YF, Zhao N. 2020. Magnetic noise enabled biocompass. *Physical Review Letters*, **124**(12): 128101.

Xie C. 2022. Searching for unity in diversity of animal magnetoreception: from biology to quantum mechanics and back. *The Innovation*, **3**(3): 100229.

Yang J, Tan GQ, Zhang T, White RH, Lu JX, Ding HG. 2015. Deletion of the proposed iron chaperones IscA/SufA results in accumulation of a red intermediate cysteine desulfurase IscS in *Escherichia coli*. *Journal of Biological Chemistry*, **290**(22): 14226–14234.

Yang PL, Cai TT, Zhang L, Yu DQ, Guo Z, Zhang YB, et al. 2022. A rationally designed building block of the putative magnetoreceptor MagR. *Bioelectromagnetics*, **43**(5): 317−326.

Zapka M, Heyers D, Hein CM, Engels S, Schneider NL, Hans J, et al. 2009. Visual but not trigeminal mediation of magnetic compass information in a migratory bird. *Nature*, **461**(7268): 1274−1277.

Zhao X, Chen HB, Lu LH, Li YQ. 2022. A mechanism of compass-free migratory navigation. *Journal of Physics D:Applied Physics*, **55**(24): 245004.